11-6-2023

System-level Noise Performance of Coherent Imaging Systems

Derek J. Burrell
University of Arizona

Joshua H. Follansbee
University of Arizona

Mark F. Spencer
Air Force Institute of Technology

Ronald G. Driggers
University of Arizona

Recommended Citation

Derek J. Burrell, Joshua H. Follansbee, Mark F. Spencer, and Ronald G. Driggers, "System-level noise performance of coherent imaging systems," Opt. Express 31, 38625-38639 (2023).

Research Article | Vol. 31, No. 23 / 6 Nov 2023 / Optics Express 38625
Optics EXPRESS

System-level noise performance of coherent imaging systems

DEREK J. BURRELL,[1,*] JOSHUA H. FOLLANSBEE,[1] MARK F. SPENCER,[2] AND RONALD G. DRIGGERS[1]

[1]The University of Arizona, Wyant College of Optical Sciences, Tucson, AZ 85721, USA
[2]Air Force Institute of Technology, Department of Engineering Physics, Dayton, OH 45433, USA
[*]derekburrell@optics.arizona.edu

Abstract: We provide an in-depth analysis of noise considerations in coherent imaging, accounting for speckle and scintillation in addition to "conventional" image noise. Specifically, we formulate closed-form expressions for total effective noise in the presence of speckle only, scintillation only, and speckle combined with scintillation. We find analytically that photon shot noise is uncorrelated with both speckle and weak-to-moderate scintillation, despite their shared dependence on the mean signal. Furthermore, unmitigated speckle and scintillation noise tends to dominate coherent-imaging performance due to a squared mean-signal dependence. Strong coupling occurs between speckle and scintillation when both are present, and we characterize this behavior by fitting a scale factor capable of generating variances in closed form. We verify each of these claims through a series of wave-optics simulations, and we see strong agreement in general between numerical results and theoretical predictions. Our findings allow us to confidently gauge signal-to-noise ratio (SNR) expectations when active illumination produces coherent noise.

1. Introduction

In designing electro-optical and infrared (EO/IR) systems, resolution and sensitivity play the most impactful roles in determining overall performance [1]. The point-spread function (PSF) and optical transfer function (OTF) of an *incoherent* imaging system fully describe its resolution in the spatial and frequency domains, respectively [2]. Analogously, the amplitude-spread function (ASF) and amplitude transfer function (ATF) provide complete descriptions of a *coherent* imaging system's resolution [3]. The metric of interest for sensitivity is often a signal-to-noise ratio (SNR) or contrast-to-noise ratio (CNR), depending on the imaging task at hand. Accurate estimates of all relevant signals and noise sources are necessary to make such calculations, and considerable effort has gone into radiometric analysis and scaling-law modeling with this very goal.

As a prominent example of imager modeling, the U.S. Army Night Vision and Electronic Sensors Directorate (NVESD) maintains the Night Vision Integrated Performance Model (NV-IPM) to evaluate resolution and sensitivity among many other outputs. Though initially conceived with only passive imaging in mind, the model has grown over time to include pulsed and continuous-wave active sources as well. In spite of these developments, there is no noise component to account for interference of coherent light as it scatters from an optically rough surface or propagates through a distributed-volume turbulent medium; we refer to these effects as speckle and scintillation, respectively [4].

It is possible to safely neglect scintillation in a physical model by assuming steep slant-path geometries or simply very low turbulence over horizontal paths. Assuming space-to-ground imaging in the former case, there is limited propagation distance following phase perturbations for scintillation to occur since turbulence is primarily concentrated near the aperture (i.e., at the earth's surface). The absence of speckle effects is particularly problematic, however, as the usual simplifying assumption of a Lambertian surface in radiometric calculations necessarily implies

#504372 https://doi.org/10.1364/OE.504372
Journal © 2023 Received 28 Aug 2023; revised 2 Oct 2023; accepted 2 Oct 2023; published 31 Oct 2023

Optics EXPRESS

diffuse backreflections. As we will see, speckle noise is often so pronounced that it becomes the limiting factor in coherent imaging performance.

There does not currently appear to be a comprehensive, system-level treatment of imaging sensitivity that covers both conventional and coherent noise anywhere else in the peer-reviewed literature. Riker *et al.* proposed a simple expression for speckle SNR that varies directly with normalized object size [5,6] based on technical reports analyzing three-bar targets [7,8]. In their examples, the total SNR is then an inverse quadrature sum of the speckle and radiometric SNRs. In a similar vein, Andrews *et al.* suggested an effective SNR that goes inversely as the radiometric SNR scaled by the scintillation index [9].

In our approach, we posit that an expression for effective SNR in its traditional form of a mean over a quadrature sum should be realizable on the basis of two observations: (1) that truly uncorrelated noise terms (whether additive or multiplicative) always add up in quadrature, and (2) that dependence on a common variable doesn't necessarily imply correlation. With that said, the next section presents analytical expressions for both conventional and coherent noise before exploring possibilities for mutual coupling between them. The sections beyond that introduce a wave-optics simulation methodology for the purpose of verifying theory, compare the theory against numerical results, and make recommendations as to proper treatment of system-level noise in coherent imaging.

2. Noise theory

In what follows, we first offer a brief review of conventional noise sources in digital imagery. Namely, these noise sources include photon shot noise, dark shot noise, and read noise. After introducing each and explaining their quadrature addition, we move on to discussing the coherent noise sources that are central to the theme of this paper: speckle and scintillation. We tabulate straightforward analytical expressions, reinterpreted from a literature review, that can predict respective noise values due to speckle or scintillation alone. We then pose the question of whether such coherent noise is subject to quadrature addition with conventional sources, and under which conditions if so. As is customary in this sort of analysis, we take all noise calculations to be in an image plane on a per-pixel basis.

2.1. Conventional noise sources

The quantum properties of light give rise to natural photon fluctuations about the average signal reaching a detector. Being a discrete process, this fluctuating behavior obeys Poisson statistics where the variance is equal to the mean arrival rate. Shot noise associated with photodetection is therefore related to the mean spectral signal $\langle Q(\lambda)\rangle$ in units of photons [γ] by

$$\begin{aligned}\sigma_{\mathrm{ps}}(\lambda) &= \sqrt{\langle Q(\lambda)\rangle} \\ &= \sqrt{\eta(\lambda)\left\langle E_{\mathrm{q}}(\lambda)\right\rangle \tau \mathcal{A}_{\mathrm{p}}},\end{aligned} \tag{1}$$

where σ_{ps} is a standard deviation in photoelectrons [e^-] at wavelength λ [m], η is the detector quantum efficiency [e^-/γ], $\langle E_{\mathrm{q}}(\lambda)\rangle$ is the mean *actinometric* irradiance [$\gamma/\mathrm{s/m}^2$], τ is the camera integration time [s], and $\mathcal{A}_{\mathrm{p}}$ is the detector pixel area [m^2]. We also note that $\langle E_{\mathrm{q}}(\lambda)\rangle = \langle E_{\mathrm{e}}(\lambda)\rangle \div (hc/\lambda)$, where $\langle E_{\mathrm{e}}(\lambda)\rangle$ is the mean *energetic* irradiance [$\mathrm{W/m}^2$], h the Planck constant [$\mathrm{J}\cdot\mathrm{s}$] and c the speed of light [m/s]. Often it is convenient to estimate total photon noise (and thus the signal itself) by evaluating Eq. (1) under the assumption of quasimonochromatic light at central wavelength $\bar{\lambda}$, eliminating any spectral dependence such that

$$\begin{aligned}\sigma_{\mathrm{ps}} &= \sqrt{\bar{\eta}\left\langle \bar{E}_{\mathrm{q}}\right\rangle \tau \mathcal{A}_{\mathrm{p}}} \\ &= \sqrt{\langle \bar{Q}\rangle}.\end{aligned} \tag{2}$$

Optics EXPRESS

In the above,

$$\bar{\eta} = \frac{1}{\lambda_{\mathrm{hi}} - \lambda_{\mathrm{lo}}} \int_{\lambda_{\mathrm{lo}}}^{\lambda_{\mathrm{hi}}} \eta\left(\lambda\right) d\lambda \tag{3}$$

and

$$\left\langle \bar{E}_{\mathrm{q}} \right\rangle = \int_{\lambda_{\mathrm{lo}}}^{\lambda_{\mathrm{hi}}} \frac{\langle E_{\mathrm{e}}\left(\lambda\right)\rangle}{hc/\lambda} d\lambda \tag{4}$$

are the average quantum efficiency and band-integrated irradiance with λ_{lo} and λ_{hi} being the passband cut-on and cut-off wavelengths, respectively. This assumption is especially valid for active imaging systems, which tend to operate over finite spectral bands for coherence purposes (and filter down accordingly to preserve sensitivity). As an aside, coherent noise arising from interference depends on the mean incoming signal level as well. We will therefore revisit the subject of photon shot noise when we move on to discuss coupling in Section 2.3.

Moving on to the charge domain, photoelectrons intermix with thermal electrons originating from sensor electronics as they heat up during exposure. This time-dependent charge buildup in the pixel well occurs independently of any signal accumulation, comprising a pedestal of dark current with its own associated shot noise. The discrete nature of electron counting induces statistical variations that also follow a Poisson distribution, by which

$$\sigma_{\mathrm{ds}} = \sqrt{i_{\mathrm{d}}\tau}. \tag{5}$$

Here, σ_{ds} is a standard deviation in electrons [e^-] while i_{d} is the time-average dark current [e^-/px/s], which manufacturers of focal plane arrays (FPAs) usually specify.

Unlike the previous instances of time-dependent shot noise, each detector readout event produces a fixed level of read noise denoted as σ_{rd} [e^-]. FPA datasheets generally specify this RMS value as well to account for several physical processes inherent in the readout integrated circuit (ROIC) electronics, including pixel (i.e., Johnson) noise, reset (i.e., *kTC*) noise, and flicker (i.e., 1/*f*) noise. Read noise is typically Gaussian distributed with zero mean. We choose to stop here and work in the charge domain as we are not considering any post-readout sources of noise in the signal chain. Ultimately the ROIC converts all charges to digital numbers (DNs) set by the camera gain factor K [e^-/DN], constituting a digital signal; working in either domain would thus give equivalent SNRs as unitless ratios.

Taken together, the total effective noise up to this point is

$$\begin{aligned} \sigma_{\mathrm{eff}} &= \sqrt{\sigma_{\mathrm{ps}}^2 + \sigma_{\mathrm{ds}}^2 + \sigma_{\mathrm{rd}}^2} \\ &= \sqrt{\left\langle \bar{Q} \right\rangle + i_{\mathrm{d}}\tau + \sigma_{\mathrm{rd}}^2}. \end{aligned} \tag{6}$$

In other words, Eq. (6) represents an observed nose level conditioned on a mean irradiance level. It is worth pointing out here that Gaussian noise is additive in nature, whereas Poisson noise is multiplicative with stationary increments [10]. Taking their quadrature sum as in Eq. (6) is the clear path forward as all terms are mutually uncorrelated and only one is signal dependent. The question now becomes whether coherent noise (i.e., speckle and scintillation) which also shares a signal dependence might reasonably add in quadrature with conventional noise. With that in mind, we proceed by deriving similar noise variances characteristic of speckle and scintillation.

2.2. Coherent noise sources

Our goal in this section is to establish analytical expressions for coherent noise in the charge domain. We define coherent noise broadly as interference due to propagation of coherent light in both a spatial and temporal sense. Our interests include noise due to speckle (σ_{sp}) and scintillation

Optics EXPRESS

(σ_{sc}), as well as the total coherent noise (σ_{ch}) due to their combined effect. Assuming no coupling between this coherent noise and the aforementioned conventional noise, we would then propose

$$\sigma'_{eff} = \sqrt{\sigma_{ps}^2 + \sigma_{ds}^2 + \sigma_{rd}^2 + \sigma_{ch}^2} \tag{7}$$

for use in the denominator of an SNR calculation to predict noise performance of coherent imagery.

2.2.1. Noise due to speckle

Speckle is a result of rough-surface scattering, which scrambles the phase of otherwise coherent light such as emission from a laser, followed by propagation to some observation plane where interference patches form. To assess the severity of image-plane speckle noise, we turn to known expressions for partially developed speckle contrast C. In general C is a ratio of standard deviation to mean irradiance of a speckle field, such that

$$\sigma_{sp} = C\left\langle \bar{Q} \right\rangle \tag{8}$$

relates speckle contrast and mean signal level to absolute speckle noise. Irradiance follows negative-exponential statistics in a fully developed speckle pattern, meaning signal fluctuations are equal in magnitude to the mean signal itself (i.e., C goes to unity). When we mitigate speckle by any of several mechanisms, however, C is less than one and the pattern is only partially developed. Our immediate goal, then, is to attain a generalized expression for C that applies to various active imaging scenarios.

Solving for C in Van Zandt's validated analysis of modified speckle contrast [11] leads to the result

$$\begin{aligned} C &= \left(\frac{1+\mathcal{P}^2}{2}\right)^{1/2} \left\{1 + \sqrt{\left|\sqrt{1 + \frac{8\left[\pi\sigma_h \Delta\lambda \cos(\varphi)\right]^2}{\bar{\lambda}^4}} - 1\right|^2 + \left|\frac{3.5\bar{\lambda}Z_1 \tan(\varphi)}{Dl_c}\right|^2}\right\}^{-1/2} \\ &\approx \left(\frac{1+\mathcal{P}^2}{2}\right)^{1/2} \left\{1 + \sqrt{\left|\frac{4\left[\pi\sigma_h \Delta\lambda \cos(\varphi)\right]^2}{\bar{\lambda}^4}\right|^2 + \left|\frac{3.5\bar{\lambda}Z_1 \tan(\varphi)}{Dl_c}\right|^2}\right\}^{-1/2}, \end{aligned} \tag{9}$$

where $\mathcal{P}$ is the backscattered degree of polarization (i.e., a ratio of polarized to unpolarized intensity), σ_h is the surface-height standard deviation, $\Delta\lambda$ is the source's $1/e$ spectral linewidth about a central wavelength $\bar{\lambda}$, φ is the object's out-of-plane tilt orientation, Z_1 is the longitudinal distance between object and entrance-pupil planes, D is the entrance-pupil diameter, and l_c is the light source's coherence length. The leading factor in Eq. (9) represents contrast due to polarization, while the first and second terms within the radical sign account for interaction of finite linewidths with surface roughness and surface tilt, respectively. Note that second line of Eq. (9) makes use of the binomial approximation for a somewhat simplified result.

In the case of unresolved *sampling-limited* imagery, we must further consider the effects of pixel averaging on speckle contrast. Assuming the equivalent *diffraction-limited* image would be well resolved, the coherence area associated with image-plane speckle is [12]

$$\mathcal{A}_c = \frac{\bar{\lambda}Z_2}{\mathcal{A}_s}. \tag{10}$$

Here, Z_2 is the longitudinal distance between exit-pupil and image planes, while $\mathcal{A}_s$ is the area of the exit pupil itself. Given a pixel integration area $\mathcal{A}_p$, speckle contrast reduces by a factor of

Optics EXPRESS

$\sqrt{\mathcal{A}_p/\mathcal{A}_c}$ when $\mathcal{A}_c < \mathcal{A}_p$, with this factor being no less than 1 as there is always a minimum of one speckle per pixel [13].

In the interest of maximizing applicability, we can recast all mechanisms of contrast reduction in terms of individual factors used to calculate speckle noise as

$$\sigma_{sp} = \left(\frac{NPX}{1 + \sqrt{B_{rgh}^2 + B_{tlt}^2}} \right)^{1/2} \langle \bar{Q} \rangle \tag{11}$$

where $X = 1$ for well-resolved imagery. With the exception of N, we break these factors down in Table 1 where pixel averaging is now cast in such a way that $X \leq 1$. For our purposes, N is the number of uncorrelated speckle frames averaged within a single camera integration time; we refer the reader to [14,15] for a framework to calculate N from known system dynamics. It is clear at this point that narrowband (i.e., temporally coherent) and linearly polarized illumination with $\Delta\lambda \to 0$, $l_c \to \infty$ and $\mathcal{P} \to 1$ indicates unit contrast. At the other extreme, broadband (i.e., temporally incoherent) and unpolarized illumination with $\Delta\lambda \to \infty$, $l_c \to 0$ and $\mathcal{P} \to 0$ becomes virtually speckle free. Shorter wavelengths also imply less speckle noise overall, which is consistent with $\bar{\lambda} \to 0$ marking the geometrical-optics limit where there is no interference and, in turn, no speckle.

Table 1. Speckle-reduction factors used in calculations of absolute coherent noise.

quantity	symbol	expression
band-averaging roughness factor	B_{rgh}	$[2\pi\sigma_h \Delta\lambda \cos(\varphi)/\bar{\lambda}^2]^2$
band-averaging tilt factor	B_{tlt}	$3.5\bar{\lambda}Z_1 \tan(\varphi)/(D_{EP} l_c)$
polarization-averaging factor	P	$(1 + \mathcal{P}^2)/2$
pixel-averaging factor (unresolved)	X	$[2\bar{\lambda}Z_2/(pD_{XP})]^2/\pi$ (circular aperture) $[\bar{\lambda}Z_2/(pD_{XP})]^2$ (square aperture)

2.2.2. Noise due to scintillation

Scintillation occurs when the turbulent atmosphere introduces phase and/or amplitude distortions along the path of a traveling wavefront, resulting in irradiance fades that degrade SNRs. With added propagation distance past these distortions, phase perturbations give rise to amplitude fluctuations and vice versa; thus, scintillation is most severe in the case of long-range imaging across a distributed volume of turbulence (as in a horizontal path). It is common to gauge the "strength" of scintillation by the Rytov number ($\mathcal{R}$) or Rytov variance ($\sigma_R^2 = 4\mathcal{R}$), which in weak-to-moderate conditions (corresponding to $\sigma_R^2 \lesssim 1$) approximate the log-amplitude variance (σ_χ^2) and log-irradiance variance ($\sigma_{\ln I}^2 = 4\sigma_\chi^2$), respectively [9]. Also assuming weak scintillation, the log-irradiance—and therefore Rytov—variance approximates the normalized irradiance variance a.k.a. scintillation index ($\sigma_I^2 = \sigma_{\bar{Q}}^2/\langle \bar{Q} \rangle^2 = \exp(4\sigma_\chi^2) - 1 \approx \exp(4\mathcal{R}) - 1 \approx 4\mathcal{R}$). Thus if we estimate the scintillation index from Rytov number, we can predict absolute scintillation noise to be

$$\sigma_{sc} = \sqrt{\sigma_I^2} \langle \bar{Q} \rangle . \tag{12}$$

Again in the case of *sampling-limited* unresolved imagery, we must consider the effects of aperture averaging on optical scintillation. To a first order, we can quantify this image-plane scintillation index as the pupil-plane expression modified by an aperture-averaging factor $A \leq 1$. Andrews has provided interpolation formulae for such effects [16] as functions of the Fresnel

Optics EXPRESS

number

$$N_{\mathrm{F}} = \frac{(D/2)^2}{\bar{\lambda} Z_1}, \tag{13}$$

since scintillated correlation widths are on the order of the first Fresnel zone radius $\sqrt{\bar{\lambda} Z_1}$ and N_{F} counts the number of Fresnel zones contained within the entrance pupil. Scintillation index reduces further through the use of polychromatic light, which Fante [17] and Baykal [18] have both shown to produce a bandwidth-averaging factor that applies to either spherical- or plane-wave illumination. Korotkova [19] more recently demonstrated how scintillation scales with polarization in the same way as speckle [cf. Eq. (9)].

In effect, scintillation decreases by all the same mechanisms as speckle except surface roughness which does not apply to turbulent media. Restricting our attention to the regime of weak-to-moderate turbulence (i.e., before scintillation begins to saturate), we proceed to recast all physical processes that affect the scintillation index such that

$$\sigma_{\mathrm{sc}} = 2\,(\mathcal{R} A B N P)^{1/2} \left\langle \bar{Q} \right\rangle \tag{14}$$

where $A = 1$ for well-resolved imagery and N is again the number of averaged frames over a long exposure. Table 2 lists each of these factors; we state plane-wave expressions for completeness but prefer the spherical-wave versions in practice, as they agree well with our simulation results and infinite plane-wave analysis is known to poorly approximate horizontal-path imaging anyhow [20]. The above relationships suggest that longer wavelengths, shorter propagation paths, larger aperture sizes (when unresolved), broader bandwidths and greater depolarization all contribute to reduced scintillation. Its wavelength dependence is not strictly monotonic, however, due to $\bar{\lambda}$ appearing multiple places in the expression. We note that this analysis only covers scintillation on the downlink path, neglecting the effects of uplink scintillation. Andrews *et al.* derive more complete expressions for scintillation index concerning two-way propagation from either a monostatic or bistatic system [9].

Table 2. Scintillation-reduction factors in calculations of absolute coherent noise.

quantity	symbol	expression
Rytov number	$\mathcal{R}$	$0.124 C_n^2 k^{7/6} Z_1^{11/6}$ (spherical wave) $0.307 C_n^2 k^{7/6} Z_1^{11/6}$ (plane wave)
aperture-averaging factor (unresolved)	A	$(1 + 1.54 N_{\mathrm{F}}^{5/6})^{-7/5}$ (spherical wave) $(1 + 6.67 N_{\mathrm{F}})^{-7/6}$ (plane wave)
bandwidth-averaging factor	B	$1 - 0.445(\Delta\lambda/\bar{\lambda})^{5/6}$
polarization-averaging factor	P	$(1 + \mathcal{P}^2)/2$

2.3. Coupled noise effects

With noise parameters defined in the isolated cases of either speckle or scintillation, we now turn our attention to whether their shared dependence on mean signal level gives rise to correlation with photon noise. Recalling that photoevents are in general Poisson distributed, the conditional probability mass function (PMF) describing photon noise is [21]

$$P\left(K|\bar{Q}\right) = \frac{\bar{Q}^K}{K!} \exp\left(-\bar{Q}\right) \tag{15}$$

where K represents the quantum photoevent count and $\bar{Q}$ is the classical energy accumulated at each point in the image. We are ultimately interested in an unconditional variance of photoelectron

Optics EXPRESS

arrival, which the law of total variance dictates is [22]

$$\mathrm{Var}\left[K\right] = \mathrm{E}\left[\mathrm{Var}\left[K|\bar{Q}\right]\right] + \mathrm{Var}\left[\mathrm{E}\left[K|\bar{Q}\right]\right]. \tag{16}$$

Here, $\mathrm{E}\left[\circ\right]$ denotes an expected value and $\mathrm{Var}\left[\circ\right]$ a variance. From Eq. (15),

$$\begin{aligned}\mathrm{E}\left[K|\bar{Q}\right] &= \sum_{K=0}^{\infty} K\frac{\bar{Q}^K}{K!}\exp\left(-\bar{Q}\right)\\ &= \bar{Q}\end{aligned} \tag{17}$$

and

$$\begin{aligned}\mathrm{Var}\left[K|\bar{Q}\right] &= \sum_{K=0}^{\infty} K^2\frac{\bar{Q}^K}{K!}\exp\left(-\bar{Q}\right) - \mathrm{E}^2\left[K|\bar{Q}\right]\\ &= \bar{Q},\end{aligned} \tag{18}$$

confirming the known property of a Poisson distribution that its sole parameter (in this case $\bar{Q}$) determines both its mean and variance.

In vacuum, speckle statistics generally obey the gamma probability density function (PDF) [12]

$$P\left(\bar{Q}\right) = \frac{\beta^\alpha}{\Gamma\left(\alpha\right)}\bar{Q}^{\alpha-1}\exp\left(-\beta\bar{Q}\right) \tag{19}$$

in canonical form with parameters $\alpha = 1/C^2$ and $\beta = 1/(C^2\langle\bar{Q}\rangle)$, where again C is the vacuum speckle contrast ratio from Eq. (9). Equations (17) and (18) imply

$$\begin{aligned}\mathrm{E}\left[\mathrm{Var}\left[K|\bar{Q}\right]\right] &= \frac{\beta^\alpha}{\Gamma\left(\alpha\right)}\int_0^\infty \bar{Q}^\alpha\exp\left(-\beta\bar{Q}\right)d\bar{Q}\\ &= \frac{\alpha}{\beta}\end{aligned} \tag{20}$$

and

$$\begin{aligned}\mathrm{Var}\left[\mathrm{E}\left[K|\bar{Q}\right]\right] &= \frac{\beta^\alpha}{\Gamma\left(\alpha\right)}\int_0^\infty \bar{Q}^{\alpha+1}\exp\left(-\beta\bar{Q}\right)d\bar{Q} - \mathrm{E}^2\left[\mathrm{Var}\left[K|\bar{Q}\right]\right]\\ &= \frac{\alpha}{\beta^2},\end{aligned} \tag{21}$$

such that

$$\begin{aligned}\sigma_{\mathrm{ps}} &= \sqrt{\frac{\alpha}{\beta} + \frac{\alpha}{\beta^2}}\\ &= \sqrt{\langle\bar{Q}\rangle + C^2\langle\bar{Q}\rangle^2}\end{aligned} \tag{22}$$

for a Poisson-gamma distribution. Note that Eq. (19) reduces to the negative-exponential PDF commonly associated with fully developed speckle when $C = 1$, while Eq. (22) converges to the incoherent result of Eq. (2) as $C \to 0$. Since noise resulting from the presence of both photon noise and speckle noise is clearly a quadrature sum, we can conclude that there is no correlation between the two despite their common dependence on $\langle\bar{Q}\rangle$. It is worth noting that speckle noise will tend to dominate over photon noise due to its stronger proportionality with $\langle\bar{Q}\rangle$, meaning substantial mitigation of speckle is required to reach the photon-noise limit.

Optics EXPRESS

In the absence of speckle but the presence of weak-to-moderate scintillation, the Rytov approximation gives rise to the lognormal PDF [23]

$$P\left(\bar{Q}\right) = \frac{1}{\bar{Q}\sigma\sqrt{2\pi}} \exp\left(-\frac{\ln\left(\bar{Q}\right) - \mu}{2\sigma^2}\right) \tag{23}$$

in canonical form with parameters $\mu = \ln(\langle\bar{Q}\rangle/\sqrt{1+\sigma_I^2})$ and $\sigma = \sqrt{\ln\left(1+\sigma_I^2\right)}$. In this case, Eqs. (17) and (18) tell us

$$\begin{aligned} \mathrm{E}\left[\mathrm{Var}\left[K|\bar{Q}\right]\right] &= \frac{1}{\sigma\sqrt{2\pi}} \int_0^\infty \exp\left(-\frac{\ln\left(\bar{Q}\right) - \mu}{2\sigma^2}\right) d\bar{Q} \\ &= \exp\left(\mu + \frac{\sigma^2}{2}\right) \end{aligned} \tag{24}$$

and

$$\begin{aligned} \mathrm{Var}\left[\mathrm{E}\left[K|\bar{Q}\right]\right] &= \frac{1}{\sigma\sqrt{2\pi}} \int_0^\infty \bar{Q} \exp\left(-\frac{\ln\left(\bar{Q}\right) - \mu}{2\sigma^2}\right) d\bar{Q} - \mathrm{E}^2\left[\mathrm{Var}\left[K|\bar{Q}\right]\right] \\ &= \exp\left(2\mu + \sigma^2\right)\left[\exp\left(\sigma^2\right) - 1\right], \end{aligned} \tag{25}$$

such that

$$\begin{aligned} \sigma_{\mathrm{ps}} &= \sqrt{\exp\left(\mu + \frac{\sigma^2}{2}\right) + \exp\left(2\mu + \sigma^2\right)\left[\exp\left(\sigma^2\right) - 1\right]} \\ &= \sqrt{\langle\bar{Q}\rangle + \sigma_I^2\langle\bar{Q}\rangle^2} \end{aligned} \tag{26}$$

for a Poisson-lognormal distribution. Once again we find no correlation between photon noise and scintillation noise, since this end result has the form of a quadrature sum between terms that share a dependence on $\langle\bar{Q}\rangle$ with no additional term containing a correlation coefficient. We also note the same proportionality with scintillation as we saw with speckle before, indicating scintillation noise will also tend to dominate over photon noise.

We now must ask the question of what happens when *both* speckle and scintillation are present in an active imaging scenario, as is often the case in horizontal-path geometries. Gudimetla and Holmes proposed the two-parameter K (a.k.a. gamma-gamma) distribution as a general model to parameterize irradiance statistics by degrees of freedom with respect to both speckle and scintillation [24]. However, they demonstrated both analytically and experimentally that normalized variance does not increase monotonically with turbulence strength in the presence of speckle [25–27]. Rather, it remains at a constant unity for very low scintillation strengths where speckle phase dominates, rises above 1 as atmospheric log-amplitude perturbations grow stronger until peaking around 1.25 for $\sigma_\chi^2 \approx 0.1$, and finally decays back down to unity as scintillation saturates and atmospheric phase perturbations take over [28]. These trends are relatively indifferent to specific beam parameters and propagation geometries [29], and they are consistent with what we've seen in our own simulations and experimental trials.

Since we cannot simply add in quadrature the theoretical expressions of Sections 2.2.1 and 2.2.2, we seek an alternative closed-form expression for the combined effects of speckle and scintillation that we encounter in active imaging. In integral form, the covariance calculations of Refs. [25–27] require involved numerical calculations to produce meaningful results. We can instead use the relatively constant shape of their normalized irradiance curves to our advantage

Optics EXPRESS

by fitting a four-parameter lognormal function of the form

$$\varsigma(\mathcal{R}) = c_1 \exp\left\{-\frac{\ln(2)}{\ln^2(c_4)} \ln^2\left[1 + \frac{(\mathcal{R} - c_2)\left(c_4^2 - 1\right)}{c_3 c_4}\right]\right\} \tag{27}$$

with $c_1 = 0.125$, $c_2 = 0.1$, $c_3 = 0.3$ and $c_4 = 3.3$ using TableCurve 2D. Figure 1 shows a semilog plot of this function, which we treat as a scale factor in calculating the coupled variance for coherent noise according to the K distribution model as

$$\sigma_{\text{ch}} = \sqrt{\left[1 + C^2\right]\left[1 + \varsigma(\mathcal{R})\right] - 1}\,\langle\bar{Q}\rangle\,. \tag{28}$$

Here, $\varsigma(\mathcal{R})$ has replaced $(4\mathcal{R})^2$ in the expression for scintillation noise variance as compared with Eq. (14). The argument of the radical sign in Eq. (28) works out to be a sum of individual variances with the product of variances, which is identical to the form of combined variances that Bufton *et al.* derived in a related problem involving ground-to-space laser ranging of a retroreflector array [30]. All told, our conditional expression for system-level coherent noise is now

$$\begin{aligned}\sigma'_{\text{eff}} &= \sqrt{\sigma_{\text{ps}}^2 + \sigma_{\text{ds}}^2 + \sigma_{\text{rd}}^2 + \sigma_{\text{ch}}^2} \\ &= \begin{cases} \sqrt{\langle\bar{Q}\rangle + i_{\text{d}}\tau + \sigma_{\text{rd}}^2 + C^2\langle\bar{Q}\rangle^2} & \text{(speckle only)} \\ \sqrt{\langle\bar{Q}\rangle + i_{\text{d}}\tau + \sigma_{\text{rd}}^2 + \sigma_I^2\langle\bar{Q}\rangle^2} & \text{(scintillation only)} \\ \sqrt{\langle\bar{Q}\rangle + i_{\text{d}}\tau + \sigma_{\text{rd}}^2 + \left\{\left[1 + C^2\right]\left[1 + \varsigma(\mathcal{R})\right] - 1\right\}\langle\bar{Q}\rangle^2} & \text{(speckle and scintillation)} \end{cases}\end{aligned} \tag{29}$$

with reference to Tables 1 and 2. We reiterate at this stage that coherent noise (which is directly proportional to the signal) will always outweigh the conventional shot noise (which is proportional to its square root) unless sufficiently mitigated by naturally occurring or deliberately engineered means.

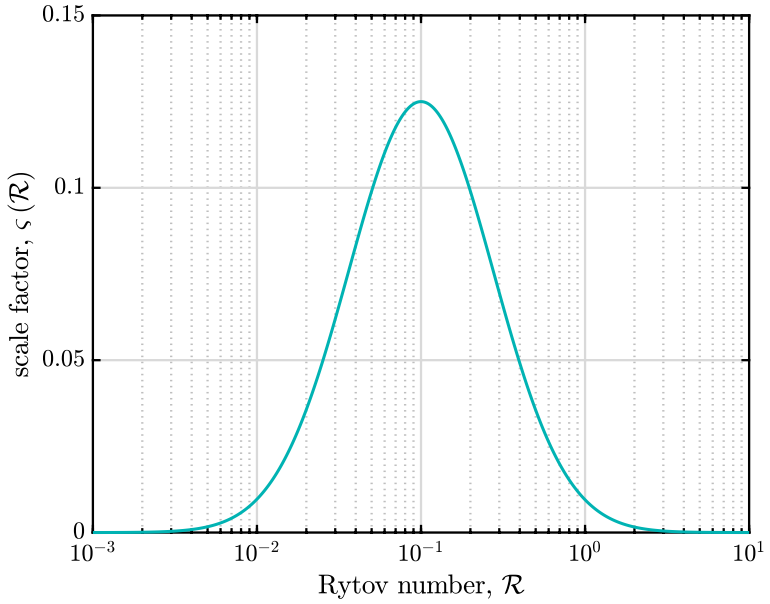

Fig. 1. Scale factor describing additional coherent noise due to scintillation when speckle noise is already present [cf. Eq. (27)].

Optics EXPRESS

3. Modeling and simulation

With the goal of verifying the theory of Section 2, we take a wave-optics simulation approach with Monte Carlo averaging to handle the stochastic nature of speckle and scintillation. To that end, we first define the amplitude of our object as a binary four-bar target on an $N \times N$ grid with each bar one-seventh as wide as it is tall. Figure 2 shows a visual of this definition, which also serves as the geometrical-optics prediction of its own image at unit magnification. With the initial amplitude of $A_0 = 1\ \sqrt{\mathrm{W}}/\mathrm{m}$ at each nonzero pixel, we update it to

$$A_0' = A_0 \sqrt{\frac{\Phi_\mathrm{e}}{\sum_{x=1}^{N} \sum_{y=1}^{N} A_0^2 (x, y)\, \delta^2}} \tag{30}$$

where Φ_e is the optical source power $[\mathrm{W}/\mathrm{m}^2]$ and δ our simulation grid spacing [m]. Going forward, we will say for simplicity that δ matches simulated pixel pitch p.

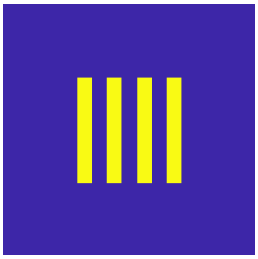

Fig. 2. Amplitude mask of four-bar target for use in numerical simulations.

To simulate the effects of diffraction through a coherent optical system, we define the circular pupil in Fig. 3(a) and take its 2D discrete Fourier transform (DFT) to find the ASF in Fig. 3(b). Convolving the geometrical image in Fig. 2 with this ASF yields the diffraction-limited image in Fig. 3(c), which we take as our "noiseless" (with respect to conventional noise) and "pristine" (i.e., speckle- and scintillation-free) image to compare against various noise degradations.

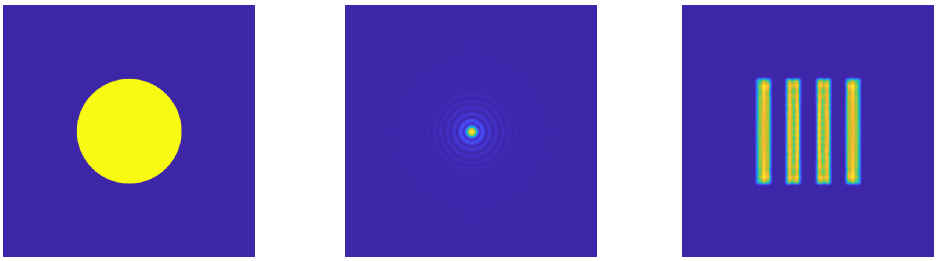

(a) (b) (c)

Fig. 3. Amplitudes of (a) circular pupil and (b) complex-valued ASF; (c) pristine coherent image of four-bar target (not drawn to scale).

From here, we take the squared modulus of our image-plane field for radiant power $[\mathrm{W}/\mathrm{m}^2]$, multiply by integration time for radiant fluence $[\mathrm{J}/\mathrm{m}^2]$, multiply by pixel area for radiant energy [J] and divide by photon energy for units of photons $[\gamma]$. We then proceed to simulate conventional noise in our diffraction-limited image. To apply photon shot noise, we generate random numbers from a pixelwise Poisson distribution with its rate parameter set to the pre-noise photon count at each pixel. Figure 4(a) shows the result of applying this noise. Multiplying by quantum

Optics EXPRESS

efficiency (η) converts this image to the charge domain, where we add a pedestal and apply a second layer of Poisson-distributed random numbers to represent dark shot noise with $i_d\tau$ setting the mean and overall rate parameter. Figure 4(b) shows the result of this step. Lastly, we add read noise in the form of random numbers drawn from a zero-mean Gaussian distribution with a standard deviation of σ_{rd}, before nullifying any negative values to zero to mimic the measurement uncertainty of a realistic analog-to-digital converter (ADC). Figure 4(c) shows our final pristine image with conventional noise degradations.

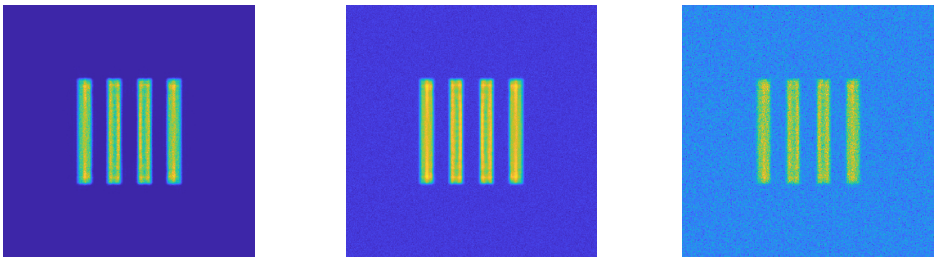

(a) (b) (c)

Fig. 4. Four-bar target image after adding simulated (a) photon shot noise, (b) dark shot noise and (c) read noise.

To simulate speckle, we define not only a flat amplitude over our four-bar target but also a uniformly distributed random phase between $-\pi$ and π. This approach rests on the assumption of δ-correlated phase on the scale at which we're simulating the object plane (i.e., $\delta \gg w_c$ where w_c is the surface-height correlation width). With the amplitude in Fig. 2 and phase in Fig. 5(a) defining the complex phasor of our object-plane field, we propagate to the pupil plane via the Fresnel diffraction integral and crop the resulting speckle field down to the pupil size as in Fig. 5(b). We then collimate this field (invoking far-field conditions) and propagate by one focal length of a thin lens to the image plane as in Fig. 5(c).

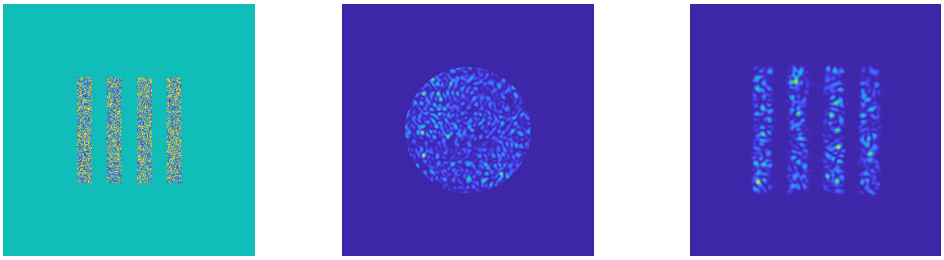

(a) (b) (c)

Fig. 5. (a) Underlying phase function of rough-surface target; resulting speckle patterns in the (b) pupil and (c) image planes (not drawn to scale).

The remaining steps between Fig. 5(c) and the speckled, conventionally noisy image in Fig. 6(a) are identical to those starting from the pristine, diffraction-limited image in Fig. 3(c). As for simulating scintillation, we revert to a flat object phase function and carry out split-step propagation through six Kolmogorov phase screens of equal strength and spacing between the object and pupil planes. We decompose the pupil-plane wavefront into Zernike modes in order to remove atmospheric tip and tilt so that the image stays roughly centered at its vacuum position [31], then propagate a second time through vacuum to arrive at the scintillated and conventionally noisy image in Fig. 6(b). Here we make note of some distortion due to anisoplanatism, but Monte

Optics EXPRESS

Carlo averaging largely alleviates any error this would introduce in our calculations. Figure 6(c) follows from the same procedure as Fig. 6(b) but begins by reinstating the δ-correlated phase of Fig. 5(a), simulating all relevant noise sources in unison. Finally, we can reuse the amplitude definition of Fig. 2 as a binary mask with any of the images in Figs. 4(c) or 6(a)–6(c) for the purpose of calculating and comparing standard deviations to test for mutual independence. Before doing so, we subtract our noiseless and pristine image in Fig. 3(c) from each to remove the influence of pure diffraction from such calculations.

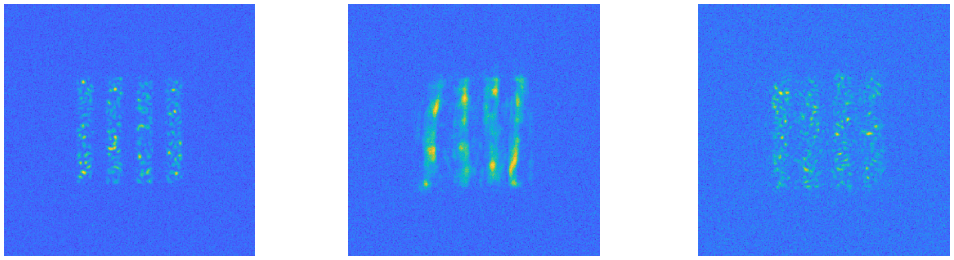

(a) (b) (c)

Fig. 6. Final image of four-bar target including all conventional noise terms in addition to (a) speckle, (b) scintillation and (c) combined speckle and scintillation.

4. Results and discussion

As an example use case, we reference the datasheet of an Allied Vision Goldeye CL-033 TEC1 for noise specifications [32]. The dark current of this particular model is 110 ke$^-$/px/s, while its read noise is 390 e$^-$ RMS. It has a quantum efficiency of 78.5% at a wavelength of 1550 nm. We assume an integration time of ~33 ms (corresponding to a 30-Hz frame rate) and set our source power to 1 mW so that various contributions to the effective noise are all on the same order of magnitude. Because it gives us a single knob to turn without affecting other parameters, we choose to vary our read noise from 0 to 400 e$^-$ in 5-e$^-$ increments while holding all other noise sources constant. We set our object size such that the object Fresnel number $N_{\text{obj}} = D/(\lambda Z_1/W) = 16$ where W is the object width; in other words, our imaging system fully resolves the object [33]. We also enforce the weak-turbulence condition that $D/r_0 = 3$, where r_0 is the Fried coherence width, leading to a spherical-wave Rytov number $\mathcal{R} = 0.06$.

The results of these tests are plotted in Fig. 7, which shows strong agreement between the theory that Eqs. (11) and (14) predict and the effective noise that we calculate from simulation data. Similarly, Fig. 8 shows promising results that suggest the scaling in Eqs. (27) and (28) provides an accurate depiction of the coupling that takes place between speckle and scintillation when both effects are present. The green line shows our working theory based on the work of Holmes *et al.* that provides good estimates. By contrast, the red lines represent alternative approaches that provide much poorer estimates: the sum of individual variances and their products from pure speckle and pure scintillation, a simple quadrature addition of the two, pure speckle only and pure scintillation only. Although not proper descriptions of the problem, the scintillation-only and speckle-only predictions do converge as the read noise surpasses the mean number of photoelectrons contained within the signal.

In addition to the radiometric calculations we present here, there is significant interest among the community in how speckle and scintillation affect SNR when the "signal" is an object's angular position rather than an optical energy. We typically quantify this track error as a noise-equivalent angle (NEA; in other words, an object angular displacement at which SNR = 1). Tyler and Fried derived an expression for NEA as a function of SNR_0, which is the radiometric

Optics EXPRESS

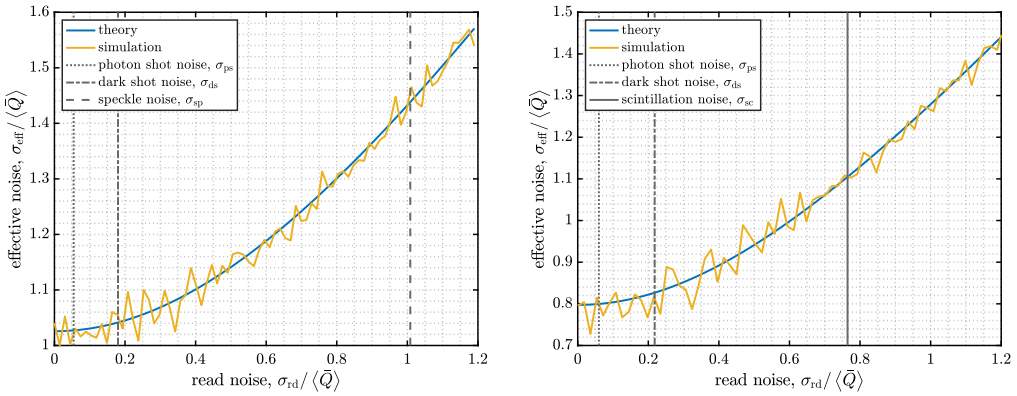

Fig. 7. Comparison of theoretical and numerical effective noise as a function of variable read noise with other conventional noise and either (a) speckle or (b) scintillation fixed; vertical lines show fixed values for reference.

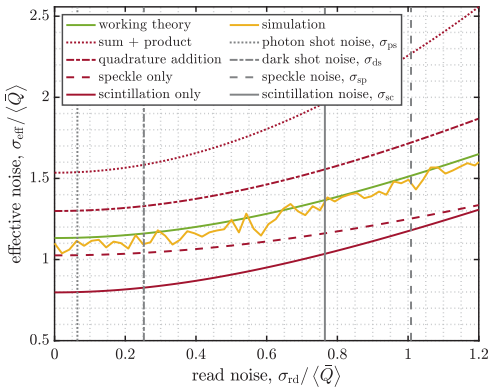

Fig. 8. Comparison of theoretical and numerical effective noise as a function of variable read noise with other conventional and coherent (speckle and scintillation combined) noise fixed; vertical lines show fixed values for reference.

SNR referring only to conventional noise (i.e., without speckle or scintillation included) [34]. Likewise, we showed in a recently published paper that the normalized NEA due to speckle depends only on object Fresnel number [35]. Although not yet approximated in closed form, Holmes published an analytical approach to finding the NEA due to scintillation as a function of beam parameters and propagation geometry; in this case it is the discrepancy between C and G tilt that manifests as track error [36]. Assuming Gaussian-distributed noise, we can expect these three error quantities to decrease in the same way as Eqs. (11) and (14) with reduced speckle contrast and root scintillation index, respectively [37]. Calling them NEA_0, NEA_{sp} and NEA_{sc}, respectively, it is therefore reasonable to assume that

$$\frac{\sigma'_\theta}{\lambda/D} = \begin{cases} \sqrt{\mathrm{NEA}_0^2 + \mathrm{NEA}_{sp}^2} & \text{(speckle only)} \\ \sqrt{\mathrm{NEA}_0^2 + \mathrm{NEA}_{sc}^2} & \text{(scintillation only)} \\ \sqrt{\mathrm{NEA}_0^2 + \left\{\left[1 + \mathrm{NEA}_{sp}^2\right]\left[1 + \varsigma\left(\mathcal{R}\right)\right] - 1\right\}} & \text{(speckle and scintillation)} \end{cases} \tag{31}$$

based on the findings of this paper.

Optics EXPRESS

5. Conclusion

This paper has developed a thorough analytic treatment of leading contributors to image noise in coherent systems. Beyond the conventional descriptions of shot and read noise, this analysis includes novel expressions for the speckle and scintillation effects that are unique to coherent imagery. We showed analytically that, when only one or the other is present, speckle and scintillation act independently of photon shot noise despite their shared dependence on mean signal strength. We verified this theory through a series of wave-optics simulations, as well as the known coupling that occurs between speckle and scintillation when both are present. By fitting a scale factor to this coupling behavior based on a literature review, we were able to account for all combinations of noise parameters within a reasonable error margin between simulation and theory. Overall, we found that coherent effects are generally dominant in assessing noise performance when left unmitigated. With validated tools in place to describe this noise performance, we can now gauge SNR and CNR expectations with greater confidence than was previously possible in coherent imaging.

Acknowledgment. D. Burrell gratefully acknowledges the Directed Energy Professional Society (DEPS) for supporting this work through a Graduate DE Research Grant Award. The views expressed are those of the authors and do not necessarily reflect the official policy or position of the Department of the Air Force, the Department of Defense, or the U.S. government. Approved for public release; distribution is unlimited. Public Affairs release approval #88ABW-2023-0726.

Disclosures. The authors declare no conflicts of interest.

Data availability. Data underlying the results presented in this paper are not publicly available at this time but may be obtained from the authors upon reasonable request.

References

1. R. G. Driggers, M. H. Friedman, and J. M. Nichols, *Introduction to Infrared and Electro-Optical Systems*, Remote Sensing Library (Artech House, Norwood, MA, 2012), 2nd ed.
2. G. D. Boreman, *Modulation Transfer Function in Optical and Electro-Optical Systems* (SPIE, Bellingham, WA, 2021), 2nd ed.
3. J. W. Goodman, *Introduction to Fourier Optics* (W. H. Freeman, New York, NY, 2017), 4th ed.
4. D. Dayton, J. Gonglewski, and C. S. Arnauld, "Laser speckle and atmospheric scintillation dependence on laser spectral bandwidth," in *Optics in Atmospheric Propagation and Adaptive Systems XII*, vol. 7476 A. Kohnle, K. Stein, and J. D. Gonglewski, eds., International Society for Optics and Photonics (SPIE, 2009), p. 74760A.
5. J. F. Riker, G. A. Tyler, and J. L. Vaughn, "Speckle imaging from an array," in *Unconventional Imaging and Wavefront Sensing XII*, vol. 9982 J. J. Dolne, T. J. Karr, and D. C. Dayton, eds. (SPIE, 2016), p. 99820J.
6. J. F. Riker, G. A. Tyler, and J. L. Vaughn, "Long-range speckle imaging theory, simulation, and brassboard results," in *Unconventional and Indirect Imaging, Image Reconstruction, and Wavefront Sensing 2017*, vol. 10410 J. J. Dolne and R. P. Millane, eds. (SPIE, 2017), p. 104100Q.
7. J. L. Vaughn, "Estimating the achieved three-bar resolution for an image that does not contain a three-bar chart," Tech. Rep. TR-935, the Optical Sciences Company, Anaheim, CA (1988).
8. G. A. Tyler, "Analysis of three bar target resolution for coherently illuminated objects," Tech. Rep. TR-1913, the Optical Sciences Company, Anaheim, CA (2015).
9. L. C. Andrews, R. L. Phillips, and C. Y. Hopen, *Laser Beam Scintillation with Applications*, vol. PM99 (SPIE, Bellingham, WA, 2001).
10. P. E. X. Silveira and R. Narayanswamy, "Signal-to-noise analysis of task-based imaging systems with defocus," Appl. Opt. **45**(13), 2924–2934 (2006).
11. N. R. Van Zandt, J. E. McCrae, and S. T. Fiorino, "Modeled and measured image-plane polychromatic speckle contrast," Opt. Eng. **55**(2), 024106 (2016).
12. J. W. Goodman, *Speckle Phenomena in Optics: Theory and Applications* (SPIE, Bellingham, WA, 2020), 2nd ed.
13. J. W. Goodman, "Statistical properties of laser speckle patterns," in *Laser Speckle and Related Phenomena*, J. Dainty, ed. (Springer-Verlag, Berlin/Heidelberg, DE, 1975), chap. 2, pp. 9–75.
14. D. J. Burrell, M. F. Spencer, N. R. V. Zandt, *et al.*, "Wave-optics simulation of dynamic speckle: I. In a pupil plane," Appl. Opt. **60**(25), G64–G76 (2021).
15. D. J. Burrell, M. F. Spencer, N. R. Van Zandt, *et al.*, "Wave-optics simulation of dynamic speckle: II. In an image plane," Appl. Opt. **60**(25), G77–G90 (2021).
16. L. C. Andrews, "Aperture-averaging factor for optical scintillations of plane and spherical waves in the atmosphere," J. Opt. Soc. Am. A **9**(4), 597–600 (1992).
17. R. L. Fante, "The effect of source temporal coherence on light scintillations in weak turbulence," J. Opt. Soc. Am. **69**(1), 71–73 (1979).

Optics EXPRESS

18. Y. Baykal, C. F. Ouyang, and M. A. Plonus, "Scintillation index for a temporally partially coherent, spherical wave light source in weak turbulence," Radio Sci. **16**(3), 343–345 (1981).
19. O. Korotkova, "Scintillation index of a stochastic electromagnetic beam propagating in random media," Opt. Commun. **281**(9), 2342–2348 (2008).
20. D. L. Fried, "Aperture averaging of scintillation," J. Opt. Soc. Am. **57**(2), 169–175 (1967).
21. J. W. Goodman, *Statistical Optics* (John Wiley & Sons, Hoboken, NJ, 2015), 2nd ed.
22. J. Blitzstein and J. Hwang, *Introduction to Probability*, Chapman & Hall/CRC Texts in Statistical Science (CRC, 2014).
23. V. P. Aksenov, V. V. Dudorov, V. V. Kolosov, *et al.*, "Probability distribution of intensity fluctuations of vortex laser beams in the turbulent atmosphere," Opt. Express **27**(17), 24705–24716 (2019).
24. V. S. Rao Gudimetla and J. F. Holmes, "Probability density function of the intensity for a laser-generated speckle field after propagation through the turbulent atmosphere," J. Opt. Soc. Am. **72**(9), 1213–1218 (1982).
25. J. F. Holmes, M. H. Lee, and J. R. Kerr, "Effect of the log-amplitude covariance function on the statistics of speckle propagation through the turbulent atmosphere," J. Opt. Soc. Am. **70**(4), 355–360 (1980).
26. C. M. McIntyre, M. H. Lee, and J. H. Churnside, "Statistics of irradiance scattered from a diffuse target containing multiple glints," J. Opt. Soc. Am. **70**(9), 1084–1095 (1980).
27. J. F. Holmes and V. S. Rao Gudimetla, "Variance of intensity for a discrete-spectrum, polychromatic speckle field after propagation through the turbulent atmosphere," J. Opt. Soc. Am. **71**(10), 1176–1179 (1981).
28. J. F. Holmes, J. R. Kerr, R. A. Elliott, *et al.*, "Experimental pulsed laser remote crosswind measurement system – feasibility study and design (part V)," Tech. Rep. ARSCD-CR-79-007, Oregon Graduate Center, Beaverton, OR (1978).
29. J. F. Holmes, "Speckle propagation through turbulence: its characteristics and effects," in *Topical Meeting on Optical Remote Sensing of the Atmosphere*, (Optica Publishing Group, 1985), p. TuB2.
30. J. L. Bufton, R. S. Iyer, and L. S. Taylor, "Scintillation statistics caused by atmospheric turbulence and speckle in satellite laser ranging," Appl. Opt. **16**(9), 2408–2413 (1977).
31. J. D. Schmidt, *Numerical Simulation of Optical Wave Propagation with Examples in MATLAB*, vol. PM199 (SPIE, Bellingham, WA, 2010).
32. Allied Vision Technologies GmbH, Stadtroda, DE, *Goldeye G/CL User Guide* (2008). V4.4.2.
33. N. R. Van Zandt, J. E. McCrae, M. F. Spencer, *et al.*, "Polychromatic wave-optics models for image-plane speckle. 1. Well-resolved objects," Appl. Opt. **57**(15), 4090–4102 (2018).
34. G. A. Tyler and D. L. Fried, "Image-position error associated with a quadrant detector," J. Opt. Soc. Am. **72**(6), 804–808 (1982).
35. D. J. Burrell, M. F. Spencer, M. K. Beason, *et al.*, "Active-tracking scaling laws using the noise-equivalent angle due to speckle," J. Opt. Soc. Am. A, preproduction (2023).
36. R. B. Holmes, "Scintillation-induced jitter of projected light with centroid trackers," J. Opt. Soc. Am. A **26**(2), 313–316 (2009).
37. G. W. Allan, R. Allured, J. Ashcom, *et al.*, "Temporally averaged speckle noise in wavefront sensors for beam projection in weak turbulence," Appl. Opt. **60**(16), 4723–4731 (2021).